JOURNAL OF MATERIALS SCIENCE 39 (2004) 997–1005

Tricalcium aluminate hydration: Microstructural observations by *in-situ* electron microscopy

P. MEREDITH*, A. M. DONALD
Polymers and Colloids Group, The Cavendish Laboratory, Department of Physics, University of Cambridge, Madingley Road, Cambridge, CB3 0HE, UK

N. MELLER‡, C. HALL
Centre for Materials Science and Engineering, The University of Edinburgh, Sanderson Building, The Kings Buildings, Mayfield Road, Edinburgh, EH9 3JL, UK
E-mail: nicola.meller@ed.ac.uk

Environmental scanning electron microscopy (ESEM) was used to study the microstructural changes that take place during the hydration of tricalcium aluminate (C_3A) in the absence and presence of gypsum ($C\bar{S}H_2$; where $A = Al_2O_3$, $C = CaO$, $H = H_2O$, $\bar{S} = SO_3$). The ESEM proves to be a valuable tool in the observation of cement hydration and no specialised equipment other than the ESEM is required. The hydration process can be observed at any time without the need to halt the hydration process prior to specimen preparation. Subsequently, artefacts associated with specimen preparation, such as water loss and desiccation, are now avoided.

In the absence of sulphate, amorphous gel, poorly crystalline hexagonal calcium aluminate hydrate (? C_4AH_{19}) and cubic calcium aluminate hydrate (C_3AH_6) are observed on the surface of C_3A grains. When small amounts of sulphate (2% gypsum) are present the same phases are observed. If larger amounts of sulphate (25% gypsum) are added to the system amorphous gel products, crystalline ettringite ($C_6A\bar{S}_3H_{32}$) and monosulphate ($C_4A\bar{S}H_{12}$) are observed. The crystalline products grow both within the amorphous gel and, where space allows, in interstices suggesting a through solution mechanism of transport.

1. Introduction

Tricalcium aluminate (C_3A) forms 5–10% of the clinker mass in ordinary Portland cement (OPC) and all hydration products of C_3A, whether or not they contain sulphate, are believed to play a key role in the induction period [1, 2]. At ordinary temperatures and in the absence of sufficient sulphate, hydration of C_3A causes a phenomenon known as 'flash set' whereby setting is accelerated by the rapid formation of hydrated calcium aluminates but the mechanical strength of the resultant paste is poor [3]. C_3A can form many hydration products in the absence of sulphate. For example:

$$2C_3A + 27H \rightarrow C_4AH_{19} + C_2AH_8$$

$$2C_3A + 21H \rightarrow C_4AH_{13} + C_2AH_8$$

$$C_4AH_{19} + C_2AH_8 \rightarrow 2C_3AH_6 + 15H.$$

In previous scanning electron microscope (SEM) studies a gel coating C_3A grains has been observed within the first ten minutes of hydration [4, 5]. The layer is of variable thickness and appears to peel off the surface [4]. Replacement of the gel by hexagonal plates occurs within one hour of hydration [5]. These plates are thought to be either C_2AH_8 or C_4AH_{13}; however laboratory X-ray diffraction (XRD) on similar pastes did not confirm the presence of either phase. After one or two hours icositetrahedra of the cubic phase C_3AH_6 are observed [4, 5], the most stable calcium aluminate hydrate at room temperature. Synchrotron X-ray diffraction suggests the formation of C_3AH_6 occurs much more quickly, the transformation from C_3A starting after only a few minutes [6]. The intermediate product has been identified as C_2AH_8 with or without C_4AH_{19}.

Addition of sulphate in the form of gypsum to the anhydrous OPC clinker suppresses these reactions by providing a source of sulphate ions. An initial gel is observed coating grains [4, 7] but it is more coherent than that observed in the absence of sulphate [4]. Ettringite rods are observed in the edge of the gel, formed by the reaction:

$$C_3A + 3C\bar{S}H_2 + 26H = C_6A\bar{S}_3H_{32}.$$

This proceeds until all the available sulphate has been used up [4]. Ettringite then reacts with remaining

Present address: Soft Condensed Matter Physics Group, Department of Physics, University of Queensland, St Lucia, Brisbane, QLD4072, Australia.
‡Author to whom all correspondence should be addressed.

C_3A to form calcium aluminium monosulphate hydrate (commonly referred to as monosulphate):

$$C_6A\bar{S}_3H_{32} + 2C_3A + (n-8)H = 3C_4A\bar{S}H_{12},$$

(where $n = 12$–14) but no such phase has been previously identified with SEM techniques.

In addition to SEM and synchrotron X-ray analysis, methods such as differential thermal analysis (DTA) [8, 9], thermogravimetric analysis (TG) [8], calorimetry [8] and X-ray diffraction (XRD) [5, 7, 10–12] have been used to examine C_3A hydration. More recently, attenuated total internal reflection Fourier transform infrared spectroscopy (ATR-FTIR) has proved useful for following the process in real time [13]. Despite all this activity, there still remains doubt as to the exact mechanism by which C_3A hydrates, both in the absence and presence of gypsum and additives. This uncertainty is not helped by the fact that standard microscopy techniques cannot provide definitive real time information regarding the formation of products and the development of morphology. Conventional light microscopy does not have the resolution to probe the microstructural events taking place in solution pores, or at grain surfaces. Conventional electron microscopy, both scanning and transmission are inherently post mortem and intrusive, due to the high vacuum observation environment.

The advent of so called 'low pressure', 'wet', 'natural state' or 'environmental' scanning electron microscopy (ESEM) has allowed *in-situ* studies to be carried out on hydrating pastes. This has a two-fold benefit in that it eliminates some of the artefacts of damaging sample preparation and allows real-time *in-situ* studies to be performed in an environment that maintains the original state of the material. The purpose of this paper is to build on previous work on Ca_3SiO_5 pastes [14, 15] by extending the *in-situ* ESEM approach to investigate the mechanism of C_3A hydration with and without gypsum.

2. Experimental details

The C_3A was supplied by Construction Technology Laboratories (CTL), Skokie, IL, code no. TJC01. The powdered material was mesh 20 and contained rough grains in the size range 0–100 μm. Reagent quality gypsum was also provided by CTL.

The *in-situ* ESEM experiments were performed on an Electroscan E3 fitted with a LaB_6 electron gun. For *in-situ* hydration experiments, a measured amount of ground dry sample, consisting of C_3A with either 0, 2 or 25% gypsum (by weight of C_3A) was placed at room temperature on the Peltier stage of the ESEM on a copper stub. The instrument was pumped down in a 'dry' sequence to prevent absorption of moisture prior to the start of observation. A chamber gas (H_2O) pressure of approximately 5 torr was set and the dry material imaged. The powder was then hydrated with a water to solid ratio (W/S) of 5 or 10 by reducing the sample temperature through the dew point. The hydration was terminated after times ranging from 30 s to 8 h and excess water removed to observe the resultant microstructure.

External hydration studies were also carried out on C_3A powders containing 25% gypsum, hydrated at W/S = 0.5 and W/S = 5. Pastes were prepared with deionised water and stored in sealed containers for 24 h. A small amount of the paste was then placed in a cooled copper stub on the Peltier stage of the ESEM at $\sim 2^\circ$C. A 'wet' pump down sequence [16] was used in order to minimise the amount of liquid exchanged between the sample and the atmosphere. Again, an imaging water vapour pressure of approximately 5 torr was set to observe the paste at 24 h.

3. ESEM observations

3.1. Hydration of C_3A in the absence of gypsum; W/S = 5

At 5 min a 'semi-transparent' amorphous coating, probably <1 μm thick, was observed on the C_3A (Fig. 1). The layer thickens with time and small plates begin to develop within this gel-coating after an hour (Fig. 2), which are probably poorly crystalline hexagonal calcium aluminate hydrates (C_2AH_8, C_4AH_{13}, C_4AH_{19}). The plates convert to the more stable cubic phase (C_3AH_6) after 8 h (Fig. 3).

3.2. Hydration of C_3A and 2% gypsum; W/S = 5

In the early stages these pastes behave similarly to those with no gypsum. An amorphous coating with foil-like morphology covers the C_3A crystals (Fig. 4) within the first few minutes. Irregular plates of calcium aluminate hydrate form within the gel in ten minutes, similar to those observed in Fig. 2.

3.3. Hydration of C_3A and 25% gypsum; W/S = 5

Within 1 min, gel-like hydration products similar to those observed in Fig. 1 form on grain surfaces. Two distinct morphologies are observed at 5 min. Proximal to gypsum grains, stubby ettringite crystals can be seen developing from the gel (Fig. 5), whilst foil-like gel, already observed for 2% gypsum (Fig. 4), develops more distally. As time passes, ettringite forms more elongate needles and the gel layer thickens. Hexagonal platelets forming rosette structures start to develop in the gel, the structures being characteristic of monosulphate. As the reaction proceeds, the formation and continued growth of existing crystallites becomes the dominant process, the C_3A grains becoming covered in a mat of ettringite crystallites (Fig. 6) whilst some primary monosulphate continues to form. After 6 to 8 h hydration small flat crystallites of secondary monosulphate grow from bundles of ettringite needles on the surface of C_3A grains (Fig. 7). In samples hydrated external to the ESEM, no monosulphate was observed, flattened splays of ettringite crystals being the dominant hydration product after 24 h (Fig. 8).

3.4. Hydration of C_3A and 25% gypsum at other W/S

When a lower W/S is used (0.5) the amount of monosulphate, both primary and secondary, is much increased. However, when a higher W/S of 10 is used

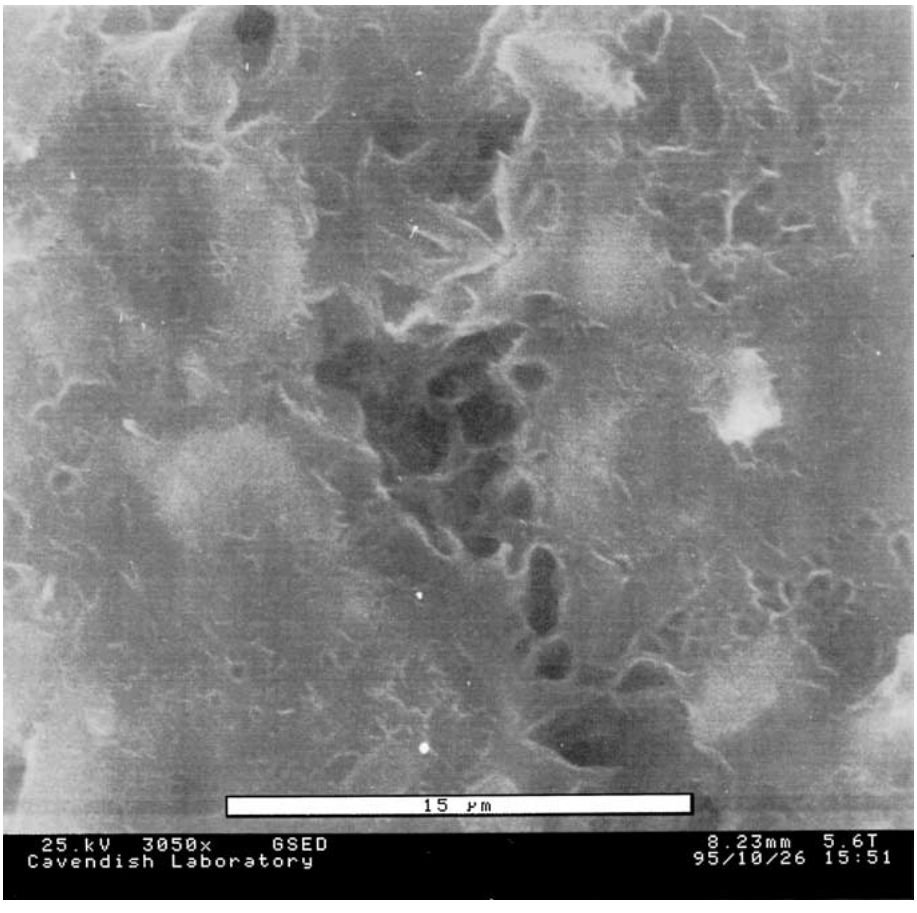

Figure 1 Amorphous gel coating a C_3A grain within the first few minutes of hydration. W/S = 5, %gypsum = 0. Scale bar is 15 μm.

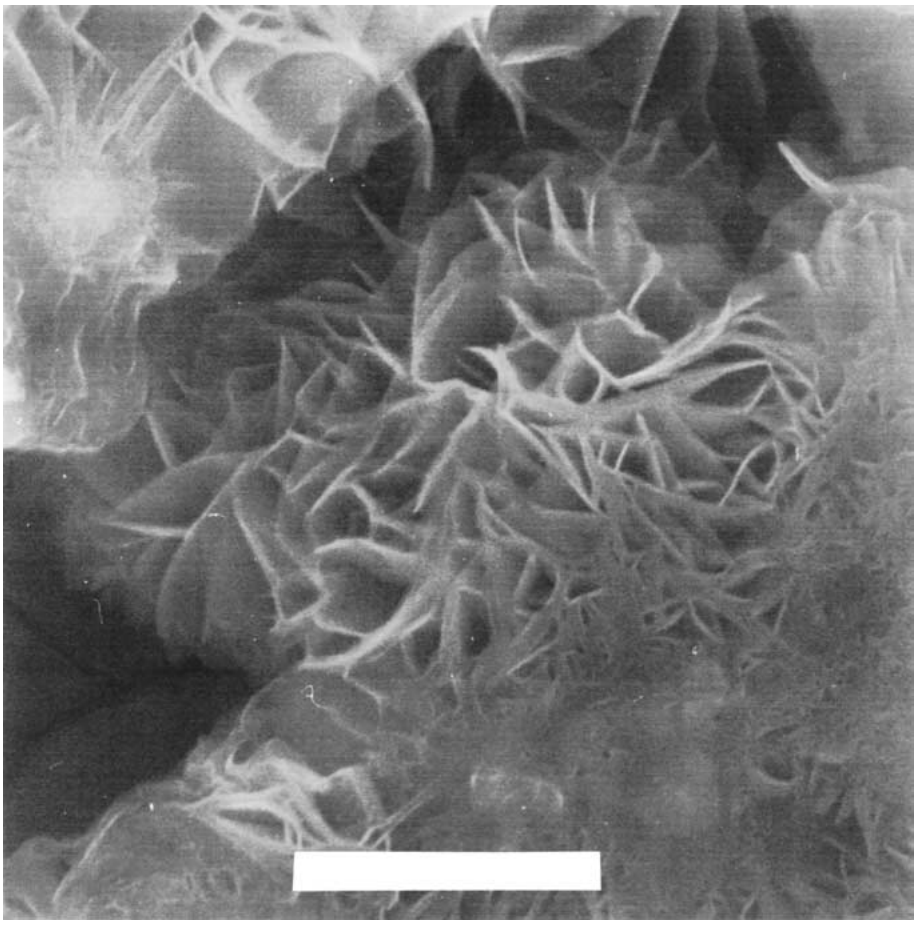

Figure 2 Hexagonal calcium aluminate hydrate plates forming in the amorphous gel on the surface of a C_3A grain. Image taken after one hour of hydration. W/S = 5, %gypsum = 0. Scale bar is 20 μm.

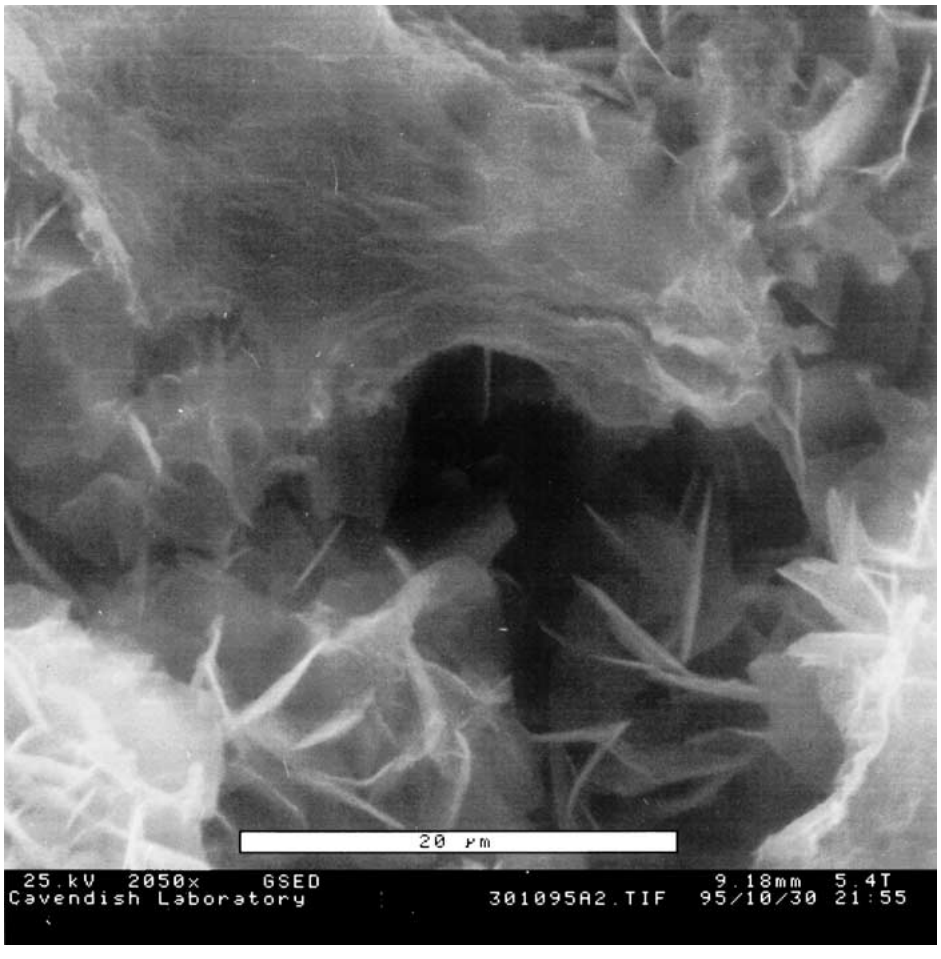

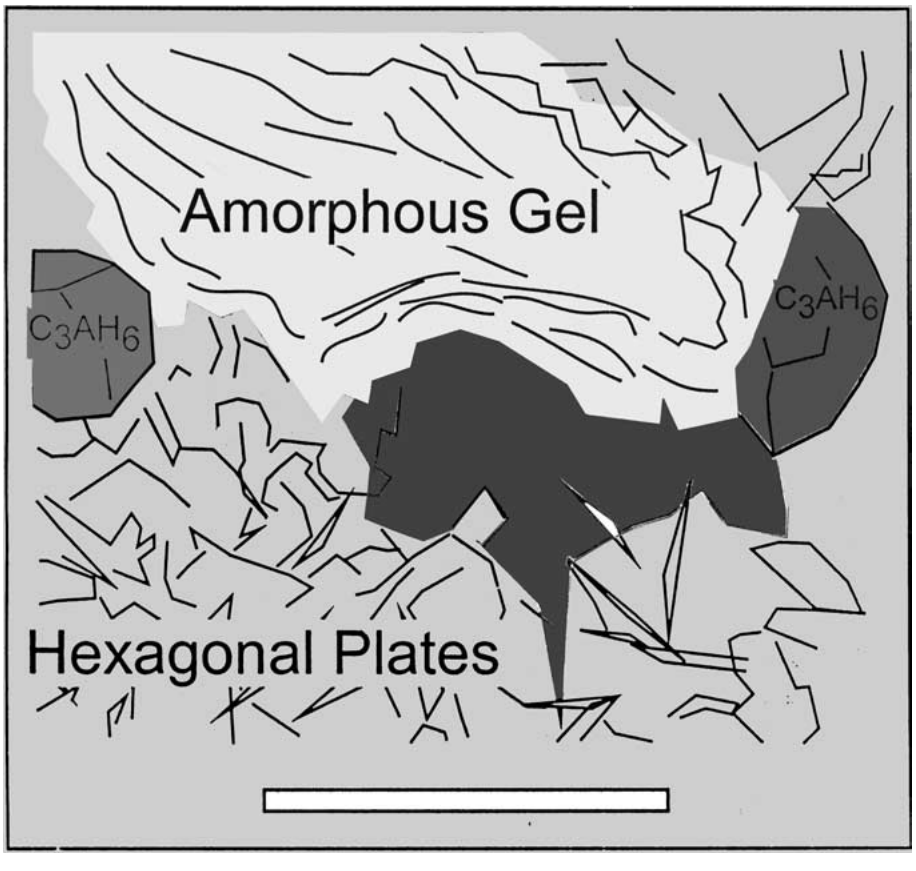

Figure 3 Micrograph and interpretative sketch of amorphous gel, hexagonal calcium aluminate hydrates and cubic C_3AH_6 on C_3A grain. Image taken after eight hours hydration. W/S = 5, %gypsum = 0. Scale bar is 20 μm.

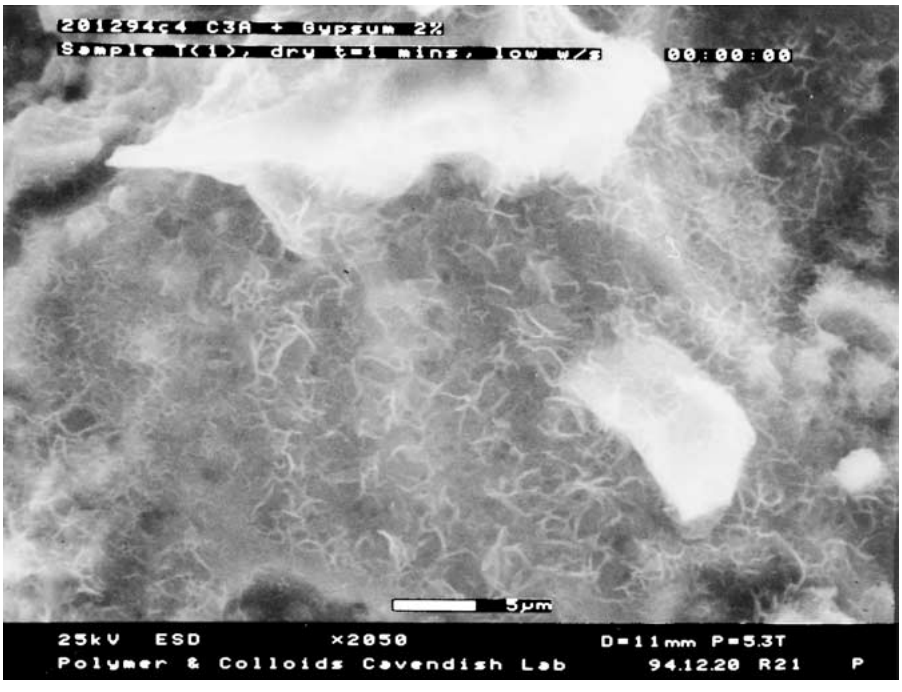

Figure 4 Foil-like gel coating C_3A grain within the first few minutes of hydration. W/S = 5, %gypsum = 2. Scale bar is 5 μm.

Figure 5 Short stubby ettringite crystals developing proximal to large gypsum crystals. Image taken after five minutes hydration. W/S = 5, %gypsum = 25. Scale bar is 5 μm.

no monosulphate is observed at all. Ettringite is the dominant hydration product and forms larger crystals (compare Figs 6 and 9) suspended in the aqueous phase in intergranular spaces.

4. Discussion

Previous SEM studies have used specialised cells to hydrate samples outside the SEM [4, 5, 7]. Using ESEM, this equipment is no longer required and the sample can be hydrated on a normal specimen holder. No time is lost at the beginning of hydration and the same sample can easily be observed at any stage of the hydration process. No coating (gold or carbon) is required in an ESEM and the usual problems associated with atmospheric CO_2 incorporation [10] are eliminated.

When little or no sulphate is present a gel coats the surface of C_3A grains (Figs 1 and 10). This gel is generally thought to inhibit further hydration and initiate the induction phase in cement, although Pratt and Scrivener [4] suggested that this gel is incoherent and even peels away from the surface of the C_3A. However, no such peeling was observed using the ESEM, suggesting the environmental chamber used by Pratt and Scrivener [4] allowed some desiccation of the sample, the 'peeling off' of the gel being a result of drying out the

Figure 6 Mats of ettringite needles covering C_3A. Image taken after 400 min of hydration. W/S = 5, %gypsum = 25. Scale bar is 5 μm.

Figure 7 Irregular platelets of secondary monosulphate forming from bundles of ettringite needles after eight hours hydration. W/S = 5, %gypsum = 25. Scale bar is 5 μm.

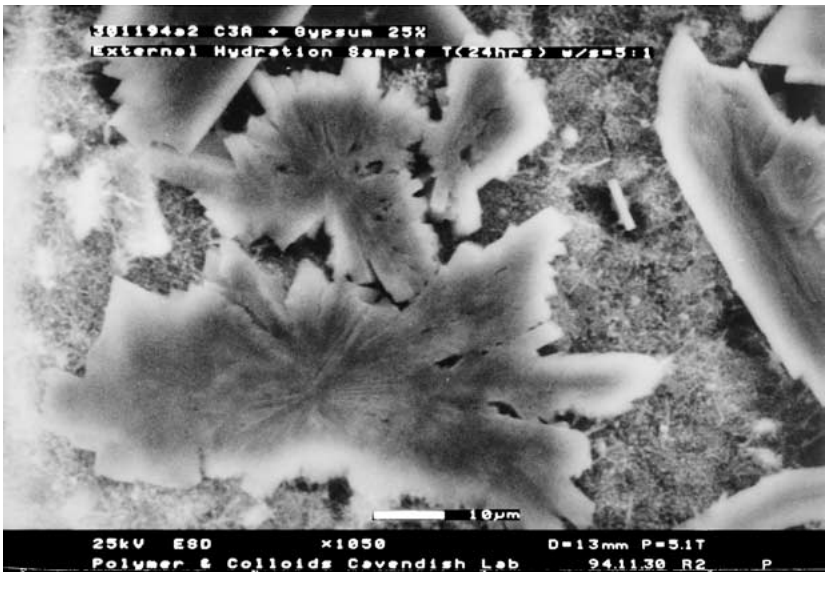

Figure 8 Splays of ettringite crystals after twenty four hours hydration external to the ESEM. W/S = 5, %gypsum = 25. Scale bar is 10 μm.

Figure 9 Long slender ettringite crystals growing in an intergranular space. W/S = 10, %gypsum = 25. Scale bar is 5 μm.

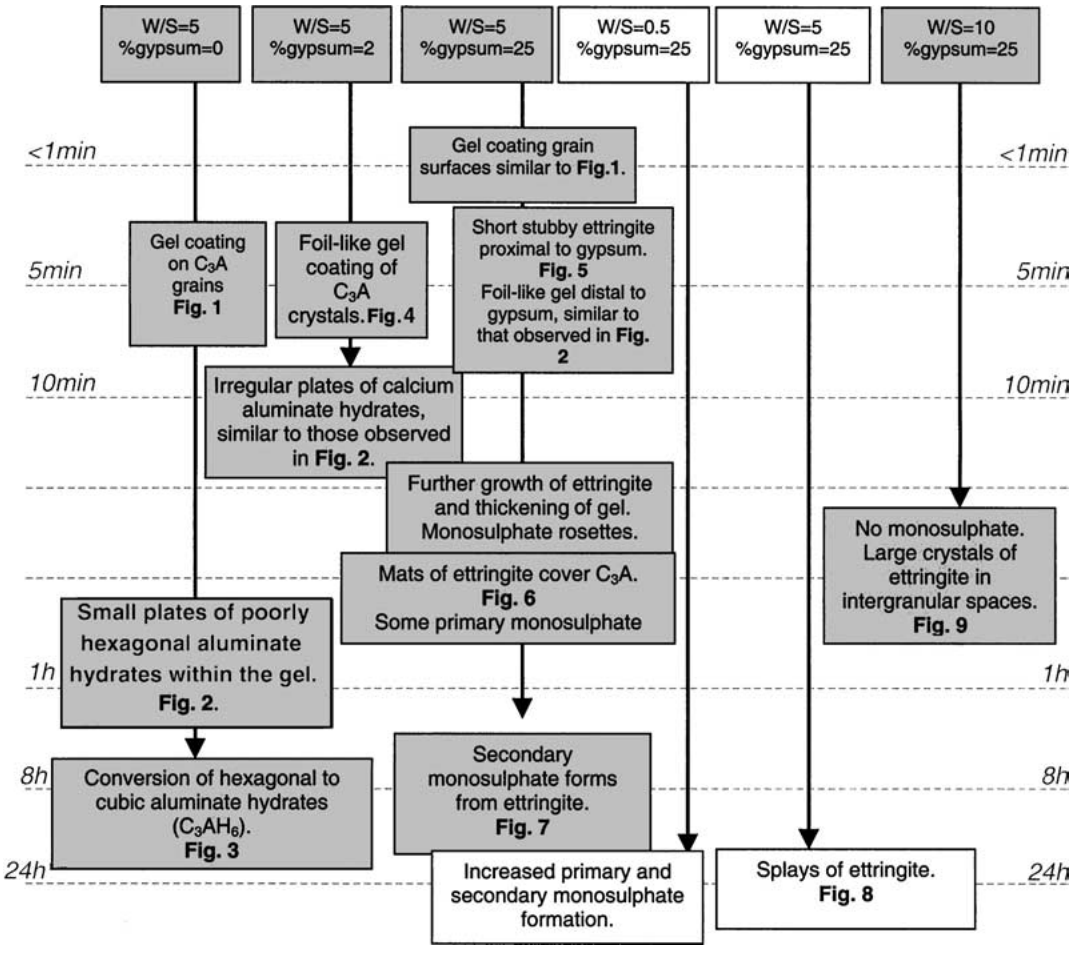

Figure 10 Summary of hydration products observed in the ESEM with various W/S ratios and gypsum additions. All gypsum additions are by weight of C_3A. Samples in grey were hydrated inside the ESEM; others were hydrated externally to the ESEM for the first 24 h.

sample. Whether the gel is capable of inhibiting further hydration is as yet debatable. Certainly it coats the C_3A grains, but calcium aluminate plates are observed within ten minutes. Microcrystalline calcium aluminates, not observable by ESEM, form even earlier as has been suggested by synchrotron X-ray analysis [6]. It is unclear from evidence here whether the plates extend down to the surface of the C_3A grains or whether a layer of gel is maintained on the C_3A surface. If a gel layer is maintained it is likely that dissolution of the C_3A grains is controlled by diffusion of ions through the gel which may slow down if not totally inhibit C_3A hydration.

Cubic aluminates (C_3AH_6) were observed amongst the calcium aluminate plates within 8 h (Figs 3 and 10). Previous SEM experiments show the formation of such cubic aluminates much earlier at 1 to 2 h [4, 5] although

the W/S ratios used in these experiments were lower than here (0.5 and <0.1, respectively, rather than 5 as used here). Synchrotron X-ray experiments suggest even more rapid C_3AH_6 formation within a few minutes although accelerated formation may occur due to localised heating by the X-ray beam [6]. The W/S is approximately 1 for Jupe *et al.*'s [6] experiment (pers. comm. C. Hall, 2002), but localised heating could have caused evaporation and reduction of the W/S, suggesting a lower W/S may speed up formation of C_3AH_6.

When only small amounts of sulphate are added to the system, calcium aluminate hydrates are still observed. However, when larger amounts are added, calcium aluminosulphate hydrates form (compare %gypsum = 2 and 25 in Fig. 10). Initially a gel is formed on C_3A as is observed in the absence of sulphate. It is likely that the gel also contains sulphate in addition to the calcium, aluminium and water. Scrivener and Pratt [4] observe that this gel was denser than that formed in the absence of sulphate. No similar observations were noted here.

Within 5 min, short stubby ettringite crystals are observed forming within the gel (Figs 5 and 10), slightly earlier than those observed by Scrivener and Pratt [4] at 10 min. The ettringite appears to grow within the gel coating C_3A grains proximal to gypsum where a source of sulphate ions is readily available. More distal to the gypsum, foil-like gel forms suggesting relatively high concentrations of sulphate are required in the early stages of ettringite formation. As time proceeds, ettringite mats cover the C_3A (Figs 6 and 10). When the W/S is increased from 5 to 10, larger crystals of ettringite are observed forming in intergranular spaces. Smaller ettringite crystals grow when the W/S is lower, although this may simply be a result of space availability. Ettringite is believed to form by diffusion [17, 18], hence where the W/S is higher there are more intergranular pores and space for new crystals to grow into [19].

The formation of primary monosulphate during the early stages of hydration has been detected by other analytical techniques. Brown and Lacroix [17] report early monosulphate when hemihydrate was used as the sulphate source, although in previous SEM studies monosulphate formation was not observed when either gypsum or hemihydrate were used, even after 4 days hydration [4]. The formation of monosulphate may result from a lack of sulphate transport after initial ettringite has formed. Areas deficient in sulphate then develop monosulphate. This argument is also supported by the fact that no monosulphate is observed when the W/S is increased from 5 to 10. A higher fluid to solid ratio would result in enhanced ion transport. In this situation no primary monosulphate is observed.

Other techniques such as calorimetry, differential thermal analysis (DTA) and infrared spectroscopy do not detect primary monosulphate. This may either be a result of increased W/S ratios or mixing during hydration. When the sample is placed in an ESEM it is not mixed or homogenised, whereas other techniques commonly stir the sample during or prior to analysis. If the sample is stirred, sulphate deficient 'pools' are unlikely to form, hence primary monosulphate is unlikely to form. Additionally, other phases or processes may bury the formation of monosulphate. For example, the ettringite infrared spectra may overlap the monosulphate peak when the ratio of ettringite to monosulphate is high. In calorimetry, the initial large exotherm would disguise any monosulphate formation and gypsum and monosulphate overlap when using DTA.

5. Conclusions

ESEM provides an easy technique for looking at C_3A hydration both in the presence and absence of gypsum. Apart from the ESEM itself, no specialised equipment is required. One sample may be observed throughout the hydration process without the need to look at multiple samples that have been hydrated external to the ESEM. Sample preparation such as reaction quenching and coating are no longer required. Furthermore, the experiment can take place in a CO_2 free environment and desiccation of the sample during preparation or observation can be avoided.

One unusual feature has been noticed: that of primary monosulphate formation. This may be a result of small-scale heterogeneities in the ESEM sample, whereas in practical operation a cement paste is usually stirred and homogenised, thus avoiding primary monosulphate formation.

Gels are observed coating grains of C_3A both in the presence and absence of sulphate. When sulphate is deficient the gel develops into plates of an unspecified calcium aluminate hydrate. Cubic C_3AH_6 eventually forms. It is not known whether the gel still coats the surface of C_3A grains during formation of crystalline phases.

If sulphate is present, ettringite forms within the gel. Primary monosulphate forms where heterogeneities in sulphate concentration exist, areas low in sulphate allowing monosulphate formation. When the W/S is increased ionic transport is enhanced and no primary monosulphate forms.

Ettringite crystals are shorter when the W/S is lower and longer when it is increased. However, it is not yet clear if this depends on the W/S ratio and saturation or space availability, there being more intergranular space available when the W/S is increased. Ettringite eventually converts to monosulphate as sulphate is used up.

Acknowledgements

This work was performed under the DTI Colloid Technology Programme and the authors acknowledge the joint funding from Schlumberger Cambridge Research, Unilever, ICI and Zeneca plc. We also thank Andrew Eddy of the University of Cambridge, Department of Physics and Karen Luke and Sarah Pelham of Schlumberger Cambridge Research.

References

1. J. BILLINGHAM and P. V. COVENEY, *J. Chem. Soc. Faraday Trans.* **89** (1993) 3021.
2. I. ODLER, "Lea's Chemistry of Cement & Concrete" (Butterworth Heinemann, Oxford, 2001) p. 241.
3. F. J. TANG and E. M. GARTNER, *Adv. Cem. Res.* **1** (1988) 67.

4. K. L. SCRIVENER and P. L. PRATT, *Brit. Ceram. Proc.* **35** (1984) 207.
5. E. BREVAL, *Cem. Conc. Res.* **6** (1976) 129.
6. A. C. JUPE, X. TURRILLAS, P. BARNES, S. L. COLSTON, C. HALL, D. HÄUSERMANN and M. HANFLAND, *Phys. Rev.* B **53** (1996) 14697.
7. J. G. CABRERA and C. PLOWMAN, *Adv. Cem. Res.* **1** (1988) 243.
8. M. COLLEPARDI, G. BALDINI and M. PAURI, *Cem. Conc. Res.* **8** (1978) 571.
9. W. A. CORSTANJE, H. N. STEIN and J. M. STEVELS, *ibid.* **4** (1974) 417.
10. H.-J. KUZEL and H. PÖLLMANN, *ibid.* **21** (1991) 885.
11. E. BREVAL, *ibid.* **7** (1977) 297.
12. P. GUPTA, S. CHATTERJI and J. W. JEFFREY, *Cem. Technol.* **4** (1973) 63.
13. K. LUKE, C. HALL, T. JONES, P. BARNES, X. TURILLAS and A. LEWIS, in SPE International Symposium on Oilfield Chemistry, San Antonio, Texas, USA, February 1995 (Society of Petroleum Engineering, 1995) p. 137.
14. P. MEREDITH, A. M. DONALD and K. LUKE, *J. Mater. Sci.* **30** (1995) 1921.
15. T. B. BERGSTROM and H. M. JENNINGS, *J. Mater. Sci. Lett.* **11** (1992) 1620.
16. R. E. CAMERON and A. M. DONALD, *J. Microsc.* **173** (1994) 227.
17. P. W. BROWN and P. LACROIX, *Cem. Conc. Res.* **19** (1989) 879.
18. N. TENOUTASSE, in Proceedings of the 5th International Symposium on the Chemistry of Cements, Tokyo, October 1968 (The Cement Association of Japan, Tokyo, 1969) p. 372.
19. P. K. MEHTA, *Cem. Conc. Res.* **6** (1976) 169.

Received 26 November 2002
and accepted 4 September 2003